

**Optical anisotropy and parallel energy bands in Au(110) and Cu(110) surfaces**

A. Ziane and S. Bouarab

*Laboratoire de Physique et Chimie Quantique, Faculté des Sciences, Université Mouloud Mammeri de Tizi-Ouzou, 15000 Tizi-Ouzou, Algeria*

(Received 11 November 2002; revised manuscript received 18 March 2003; published 26 June 2003)

The optical response of Au(110) and Cu(110) surfaces is calculated using the self-consistent method of linear muffin tin orbitals. The imaginary part of the dielectric function determined through electronic interband transitions presents an anisotropy with light polarized along the two directions at right angles from the [110] surfaces. This study establishes that the anisotropy does not result from a geometrical effect but from optical transitions between parallel surface bands.

DOI: 10.1103/PhysRevB.67.235419

PACS number(s): 78.68.+m, 78.20.Bh, 78.66.-w

**I. INTRODUCTION**

The investigation on surface optical properties of metals has recently gained renewed impulse with the development of the technique of the reflectance anisotropy spectroscopy (RAS). This technique, which was mainly used in semiconductor surface science,<sup>1,2</sup> has been extended successfully to metal surfaces. Within this technique one measures the difference of the reflectivity along two perpendicular directions on the surface. Using this method, the optical anisotropy in Ag, Cu, and Au (110) surfaces has been widely studied.<sup>3-15</sup> Several mechanisms may contribute to the surface-induced optical anisotropy: (i) electronic transitions between localized surface states,<sup>6,16</sup> (ii) transitions involving near-surface bulk states whose symmetry is reduced by the presence of an anisotropically reconstructed surface,<sup>17,18</sup> and (iii) surface plasmons may also affect the optical spectra.<sup>19</sup>

Although RAS is a powerful technique for probing the optical properties of surfaces, there is still a problem in the microscopic interpretation of the origin of such anisotropy. From the theoretical point of view, different methods are used to interpret the available experimental data for metal surfaces. Among these methods, one can cite the parametrized-model calculations like the so-called *swiss cheese* model<sup>3,9,20,21</sup> or the semi-infinite jellium model.<sup>22</sup> These models depend obviously on external input parameters and cannot account accurately for the surface-induced changes of the electronic structure. Recently, some *ab initio* effective one-electron calculations within density functional theory (DFT) and using the local density approximation (LDA) have been attempted<sup>23-26</sup> with reliable results. In order to go beyond the one-electron calculations, *ab initio* methods including self-energies, excitonic, and local field effects are available.<sup>27,28</sup> Unfortunately, to our best knowledge, calculations on the optical response of metal surfaces based upon such sophisticated numerical methods have not been attempted up to now. These methods are used to study semiconductor-based systems. It seems that self-energies, excitonic, and local-field effects are rather important in optical properties of semiconductors.<sup>29</sup>

In this context we have previously performed an *ab initio* study of the optical anisotropy in Cu, Au, and Ag (110) surfaces<sup>23,25</sup> through interband transitions based on energy bands calculated by using a self-consistent method of linear

muffin-tin orbitals (LMTO's). In the case of an Ag(110) surface<sup>25</sup> we found results in good agreement with the experimental anisotropies and explained their origin through surface, subsurface, and sub-subsurface interband transitions. However, for Cu(110) and Au(110) surfaces we did not give a detailed interpretation of the optical anisotropy through interband transitions involved in the Brillouin zone (BZ). On the other hand, recent investigation with new results on the surface optical properties of Au(110) were reported by using RAS measurements.<sup>13</sup> This recent experimental work on the Au(110) surface together with recent *ab initio* calculations<sup>26</sup> of the reflectance anisotropy spectra of Cu(110) has motivated this present study.

From the experimental point of view, the interpretation of the optical spectrum of Cu(110) is complicated and still subject to controversy. A sharp peak at 2.1 eV was observed in a clean surface with the RAS (Refs. 6, 8, and 10) technique and with second-harmonic generation.<sup>14</sup> This peak is sensitive to surface contamination and was assigned to electronic transitions involving surface states at the *Y* point of the surface BZ.<sup>6,8</sup> The optical spectrum of Cu(110) surface presents also two other structures at 3.6 and 4.2 eV which respond differently to O and CO adsorption.<sup>6,8</sup> The first one is quenched by adsorption in the same way as the 2.1 eV structure, while the second is less sensitive to contamination.<sup>6</sup> These optical structures were also observed in other experiments.<sup>10,18</sup> A recent RAS study<sup>15</sup> combined with angle-resolved ultraviolet photoemission spectroscopy (ARUPS) on the surface optical properties of clean Cu(110) and Cu(110)-(2×2)-O shows optical structures at 2.1 eV and 4.2 eV attributed to transitions between surface electronic states at *Y* and *X* points of the BZ.

Although investigations of the surface optical properties on Au(110) started a few decades ago, the origin of its optical anisotropy is less understood than that of (110) surfaces of Cu and Ag, two materials of similar electronic properties. One of the first works on Au(110) was performed by Kofman *et al.*<sup>30</sup> who obtained an anisotropic optical response by using electroreflectance measurements. The RAS measurements<sup>20,31</sup> in air and in an electrochemical environment<sup>32</sup> yielded negative anisotropy around 2.4 eV and a dominant positive structure at 3.6 eV. Similar results were also obtained recently through RAS experiments which have been also performed under clean ultrahigh-vacuum

conditions.<sup>33</sup> More recently, Stahrenberg *et al.*<sup>13</sup> have used the RAS technique to determine the surface dielectric anisotropy under ultrahigh-vacuum conditions of Au(110) for which they found spectral features at 1.9, 2.5, 2.8, 3.5, and 4.4 eV. In contrast to Cu(110) and Ag(110) surfaces, for Au(110) the agreement between RAS measurements and surface-local-field calculations is not satisfactory.<sup>3,10,20</sup>

In this work we attempt to give a microscopic interpretation of the origin of the anisotropies observed in Cu(110) and Au(110). We also propose to determine the symmetry of the orbitals concerned by the electronic interband transitions. Our calculations are based on the self-consistent method of linear muffin-tin orbitals for which we give briefly some technical details in Sec. II. The results are presented and discussed in Sec. III, and finally Sec. IV summarizes our main conclusions.

## II. METHOD

The surface is modeled by a periodically repeated slabs consisting of seven Cu (Au) atomic layers separated by five vacuum layers. The crystal coordinates of this supercell are rotated to bring the  $[1\bar{1}0]$ ,  $[001]$ , and  $[110]$  crystal directions parallel to the  $x$ ,  $y$ , and  $z$  axes, respectively.<sup>25</sup> The unit supercell is orthorhombic with interatomic distances carried back to the experimental lattice constants<sup>34</sup> of cubic-face-centered Cu (3.61 Å) Au (4.08 Å) elements.

The optical absorption of the system is directly proportional to the imaginary part of the dielectric function  $\epsilon(\omega) = \epsilon_1(\omega) + i\epsilon_2(\omega)$ ,  $\omega$  being the photon energy. Excluding the contribution of the intraband transitions (Drude's term), which is only important at very low energy ( $\propto 1/\omega^3$ ), the optical absorption  $\epsilon_2(\omega)$  incorporates the allowed interband transitions. According to the microscopic theory of optical properties in the limit of an infinite lifetime of the excitations and at  $T=0$  K,  $\epsilon_2(\omega)$  is given by a surface integration in the Brillouin zone:

$$\epsilon_2^i(\omega) = \frac{4}{\pi\omega^2} \sum_{n,n'} \int_{\text{BZ}} \frac{|\vec{P}_{nn'}^i(\vec{k})|^2}{|\vec{\nabla}\omega_{nn'}(\vec{k})|} d\vec{S}_k, \quad (1)$$

where  $i$  denotes the polarization of the light ( $i=x,y,z$ ) and  $P_{nn'}^i(\vec{k})$  is the  $i$ th component of the dipole matrix element between the initial  $|n\vec{k}\rangle$  and final  $|n'\vec{k}\rangle$  states with eigenvalues  $E_n(\vec{k})$  and  $E_{n'}(\vec{k})$ , respectively. The BZ integration is performed by using the usual tetrahedron technique<sup>35,36</sup> where the constant surface energy is  $S = \{\vec{k}; E_{n'}(\vec{k}) - E_n(\vec{k}) = \omega_{nn'}(\vec{k}) = \omega\}$ . The details of the calculation of  $P_{nn'}^i(\vec{k})$  and  $\epsilon_2(\omega)$  in the LMTO are given elsewhere.<sup>35</sup>

The above expression (1) involves a transition probability by means of the dipole matrix elements which obey the selection rules concerning the interband transitions. The electronic structure is calculated by using the LMTO method in the atomic sphere approximation (ASA) including the combined correction.<sup>37,38</sup> The exchange and correlation potential has been treated in the LDA within the von Barth–Hedin approximation.<sup>39</sup> The calculations are performed by using an

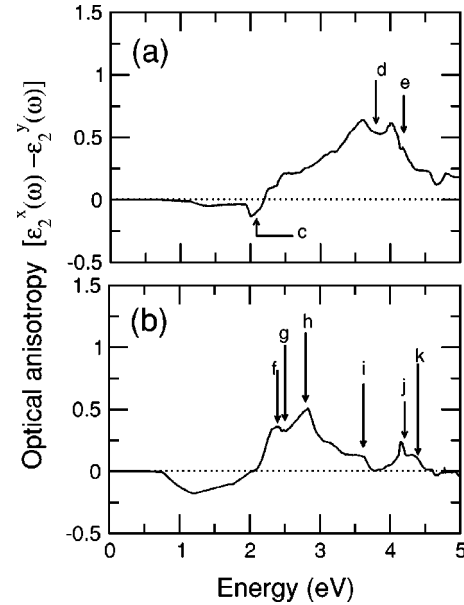


FIG. 1. Difference  $\epsilon_2^x(\omega) - \epsilon_2^y(\omega)$  between the components  $x$  and  $y$  of the imaginary part of the dielectric constant  $\epsilon_2^i(\omega)$  vs the photon energy  $\omega$  of (110) surfaces of Cu (a) and Au (b). For comparison, we have indicated by arrows the experimental peak positions: (c),(e) Refs. 6, 8, and 15, (d) Refs. 6 and 8, (f),(i),(j): Ref. 20, and (g),(h),(k) Ref. 13.

increasing number of  $k$  points in the irreducible BZ until convergence which is achieved for 578  $k$  points.

## III. RESULTS AND DISCUSSION

First, let us notice that new results concerning RAS measurements on Au(110) have been reported recently.<sup>13</sup> On the other hand, *ab initio* calculations of the RAS spectrum of Cu(110) were recently obtained by Monachesi *et al.*<sup>26</sup> where they show that the peaks observed at low energy are produced by interband transitions involving surface states whereas structures at high energy are due to transitions across bulk states.

In this present study, we will show that the calculated anisotropies are due to electronic transitions between parallel surface bands. So we focus on the energy bands along high-symmetry directions in the BZ in order to mark appropriately the location of the interband electronic transitions giving rise to the optical anisotropies. The corresponding curves to our calculated optical anisotropies in Cu and Au(110) surfaces are shown in Fig. 1. For convenience and clarity in the discussion, we report also in Table I the measured optical peak positions along with our calculated values. We denote by  $C_1$ ,  $C_2$ , and  $C_3$  the optical peaks found in the optical spectra of Cu(110) slabs for photon energies of 2.0, 3.6, and 4.0 eV, respectively. The corresponding structures of the interband transitions in Au(110) found at 1.2, 2.4, 2.8, and 4.1 eV are labeled by  $A_1$ ,  $A_2$ ,  $A_3$ , and  $A_4$ , respectively.

Figures 2 and 3 display the energy bands along high-symmetry directions in Cu(110) and Au(110), respectively, where we have marked the locations of the different optical peaks. We give the energy bands  $E(k)$  along the high-

TABLE I. The optical peak positions (eV) obtained in the present work along with available experimental and theoretical data.

	Cu			Au			
	$C_1$	$C_2$	$C_3$	$A_1$	$A_2$	$A_3$	$A_4$
Present work	2.0	3.6	4.0	1.2	2.4	2.8	4.1
Hofmann <i>et al.</i> <sup>a</sup>	2.1	3.8	4.2				
Frederick <i>et al.</i> <sup>b</sup>	2.1	3.8	4.2				
Stahrenberg <i>et al.</i> <sup>c</sup>					2.5	2.8	4.4
Mochan <i>et al.</i> <sup>d</sup>				2.4	3.6	4.2	
Monachesi <i>et al.</i> <sup>e</sup>	2.0		4.0				
Stahrenberg <i>et al.</i> <sup>f</sup>	2.1		4.2				

<sup>a</sup>Reference 6.

<sup>d</sup>Reference 20.

<sup>b</sup>Reference 8.

<sup>e</sup>Reference 26.

<sup>c</sup>Reference 13.

<sup>f</sup>Reference 15.

symmetry directions oriented by the high-symmetry points  $\Gamma$ ,  $X$ ,  $Y$ , and  $M$ .

In the supercell, when the interslab bonding is broken, for a fixed  $k$  vector in the  $(k_x, k_y)$  plane, one obtains the same eigenvalues in the  $k_z$  direction.<sup>40</sup> Therefore, in our discussion we limit ourselves only in this plane by giving the coordinates of the vectors in units of  $(\pi/a)$  and  $(\pi/b)$ . In these units the positions of the high-symmetry points  $\Gamma$ ,  $X$ ,  $Y$ , and  $M$  are  $(0,0)$ ,  $(1,0)$ ,  $(0,1)$ , and  $(1,1)$ , respectively. We use  $N(S)$ ,  $N(S-1)$ , and  $N(S-2)$  to designate the noble-metal ( $N=\text{Cu, Au}$ ) surface, subsurface, and sub-subsurface whereas  $N(V)$  is assigned to the bulklike state created in the middle of the slab.

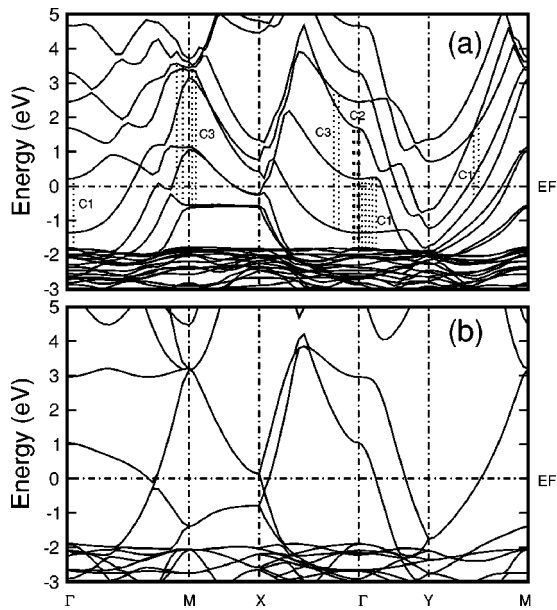


FIG. 2. Energy bands of Cu along high-symmetry directions in seven layers slab (a) and bulk (b) generated from (110) crystal coordinates. The calculated peak positions in the optical anisotropy are marked by  $C_1$ ,  $C_2$ , and  $C_3$ . The horizontal dashed line indicates the Fermi level.

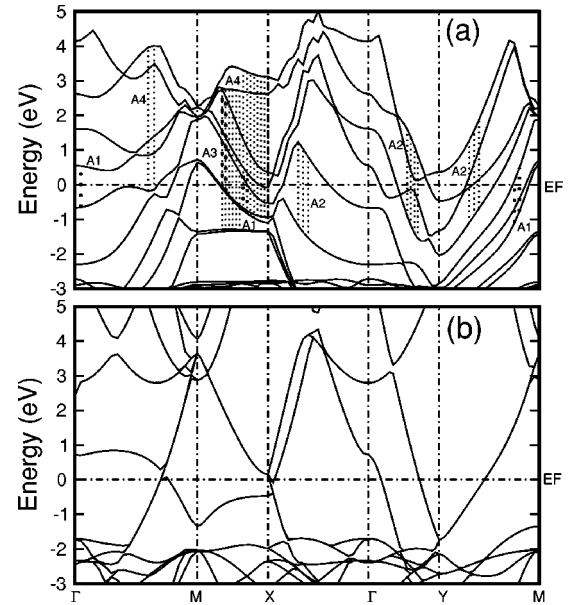


FIG. 3. Energy bands of Au along high-symmetry directions in seven layers slab (a) and bulk (b) generated from (110) crystal coordinates. The calculated peak positions in the optical anisotropy are marked by  $A_1$ ,  $A_2$ ,  $A_3$ , and  $A_4$ . The horizontal dashed line indicates the Fermi level.

First, we discuss the results of the optical structures obtained in Cu(110) through Fig. 2(a), which gives the corresponding energy bands. The first peak  $C_1$  at 2.0 eV is mainly located around  $\Gamma$  point in the  $\Gamma Y$  and  $\Gamma M$  directions. For this peak, the major contribution comes from  $\text{Cu}(S)_{d \rightarrow p}$  [denotes a transition from  $d$  to  $p$  state in the  $\text{Cu}(S)$  atomic sphere] and  $\text{Cu}(S-2)_{d \rightarrow p}$ . Beside this, there is another location of this peak around the  $(0.5, 1.0)$   $k$  point along the  $YM$  direction where the transitions are essentially due to  $\text{Cu}(S)_{s \rightarrow p}$ . The type of orbital symmetries involved and atomic layers concerned by this transition near the  $\Gamma$  point are different from those located in the  $YM$  direction. However, it seems that this structure might contain contributions arising from two different origins. The optical structure corresponding to this peak ( $C_1$ ) was observed in a number of experiments performed on the Cu(110) surface and has been found in several calculations (Table I) where its double origin is also noticed. It was assigned to electronic transitions involving surface states<sup>6,15</sup> at the  $Y$  point. Indeed, Hansen *et al.*<sup>10</sup> observed that this structure is not quenched after exposure of Cu(110) clean surfaces to air and concluded that this resonance might have two origins.

The peak  $C_2$  that we found at 3.6 eV arises from electronic transitions occurring in a very narrow region between  $(0,0,0)$  and  $(0.1,0,0)$   $k$  points in the  $\Gamma X$  direction. Its origin is due to  $d \rightarrow p$  transitions in  $\text{Cu}(S)$  and  $\text{Cu}(S-1)$ . Hofmann *et al.*<sup>6</sup> and Frederick *et al.*<sup>8</sup> have also observed a structure at 3.8 eV and have assigned it to  $d \rightarrow sp$  interband transitions.

The presence of the peak  $C_3$  (4.0 eV) results from contributions of all atomic spheres coming from different electronic transitions: ( $p \rightarrow d$ ) type in deeper layers  $\text{Cu}(S-2)$  and  $\text{Cu}(V)$  and also of ( $p \rightarrow s$ ) type in  $\text{Cu}(S)$ ,  $\text{Cu}(S-1)$ , and  $\text{Cu}(S-2)$ . It seems that this peak is due to an intrinsic an-

isotropy rather than to transitions involving only surface states. This result is in qualitative agreement with the results of Hofmann *et al.*<sup>6</sup> who found a structure around 4.0 eV which is only little affected by CO, O, and N adsorption whereas the peaks at 2.1 and 3.8 eV are rather surface sensitive. As it is shown in Fig. 2(a), this peak  $C_3$  originates from electronic transitions which occur between (0.9,0.9) and (1.0,1.0)  $k$  points in the  $\Gamma M$  direction and also between the  $M$  symmetry point up to the (1.0,0.8)  $k$  point in the  $MX$  direction.

As we can notice, the contributions of the interband transitions to the calculated anisotropies arise essentially from the three top layers ( $S$ ,  $S-1$ ,  $S-2$ ). The contribution to the peak  $C_3$  coming from the bulklike atomic layer Cu(V) is small and can be considered as negligible. The bulk atomic sphere is not significantly affected by the surface. This can be understood by the calculated charge transfer between the different atomic spheres of the slab. The most important part of the charge lost ( $0.4e^-$ ) in Cu( $S$ ) is mainly gained ( $0.3e^-$ ) by the interface empty sphere whereas the rest goes on Cu( $S-1$ ) and Cu( $S-2$ ) atomic layers. The bulklike atom Cu(V) remains neutral and it is not affected by the surface. It is clear from Fig. 2(a) that the main contributions to the interband transitions are due to parallel bands and they are not limited to only high-symmetry points.

From theoretical point of view, the optical anisotropy of Au(110) seems to be less clear. In contrast to Cu(110) and Ag(110) surfaces<sup>3,10</sup> the agreement between RAS measurements with the surface-local-field calculation assuming a bulk truncated ( $1 \times 1$ ) structure is not satisfactory.<sup>20</sup>

As we can see in Fig. 3(a), showing the corresponding energy bands of a seven-layer slab of Au(110), the electronic interband transitions giving rise to the four optical peaks  $A_1$ ,  $A_2$ ,  $A_3$ , and  $A_4$  can take place anywhere along the high-symmetry directions. Moreover, the interband transitions could not be limited to only these directions, but they could occur anywhere in the BZ. In the  $MX$  direction, the interband transitions corresponding to  $A_1$  and  $A_3$  peaks are somewhat eclipsed by the large presence of those corresponding to  $A_4$ . We have used a thick dotted line to bring up their presence. The first peak  $A_1$  at 1.2 eV appears in the three directions  $\Gamma M$ ,  $MX$ , and along  $YM$  at the (0.8,1.0)  $k$  point.

The contributions to the peak  $A_1$  located in the  $\Gamma M$  and  $MX$  directions come mainly from Au( $S-1$ ) $_{sd \rightarrow p}$  transitions, mixed with some part coming from Au( $S$ ) $_{s \rightarrow p}$ . For the last location in the  $YM$  direction, the transitions are rather of ( $sp \rightarrow sp$ ) type in Au( $S$ ).

The peak  $A_2$  at 2.4 eV located around the  $Y$  high-symmetry point along  $YM$  and  $\Gamma Y$  has its origin from Au( $S-2$ ) $_{d \rightarrow p}$ , Au( $S-1$ ) $_{d \rightarrow p}$  and Au( $S$ ) $_{s \rightarrow p}$  transitions. We found also another location around the (0.6,0.0)  $k$  point in the  $\Gamma X$  direction arising from transitions of ( $p \rightarrow s$ ) type in Au( $S-1$ ), Au( $S$ ) and of ( $d \rightarrow p$ ) type in Au( $S-2$ ).

The structure  $A_3$  at 2.8 eV is located only between (1.0,0.6) and (1.0,0.7)  $k$  points along the  $XM$  direction. Its origin comes from Au( $S$ ) $_{sd \rightarrow p}$  and Au( $S-2$ ) $_{sd \rightarrow p}$  transitions.

The peak  $A_4$  at 4.1 eV originates from (1.0,0.0) up to (1.0,0.7)  $k$  points mainly in the  $XM$  direction and also in narrow regions along the high-symmetry  $\Gamma M$  direction. A major contribution to this anisotropy comes from  $d \rightarrow p$  transitions involving the three top layers Au( $S, S-1, S-2$ ) but mainly from Au( $S$ ) $_{p \rightarrow s}$ .

As for Cu(110), we found that the bulklike layer Au(V) remains neutral whereas Au( $S$ ) loses ( $0.43e^-$ ) which is gained ( $0.33e^-$ ) essentially by its interface empty sphere. There is no contribution of Au(V) to anisotropic transitions of the Au(110) surface. It is also evident from Fig. 3(a) that the interband transitions involve mainly parallel energy bands which are not necessarily situated near high-symmetry points.

In order to shed light on the possible geometrical contribution to the optical anisotropies observed experimentally and reproduced from our calculations, we have considered a bulk Cu (Au) in the (110) direction without empty atomic spheres. Figures 2(b) and 3(b) display the energy bands of bulk Cu and Au, respectively, generated from the coordinates of the (110) crystal direction. For comparison, we have plotted the energy bands along the same high-symmetry directions as for Cu(110) and Au(110) surfaces [Figs. 2(a) and 3(a)]. When we compare Fig. 2(a) [Fig. 3(a)] with Fig. 2(b) [Fig. 3(b)], we can clearly notice that the energy bands corresponding to (110) surfaces are somewhat confined and the occupied bands are pushed towards lower energies. In the cases of bulklike (110) of the two materials [Figs. 2(b) and 3(b)], there are no parallel energy bands except for those connecting the  $\Gamma Y$  direction for which the electronic transitions are not allowed by the selection rules. So we can say that the optical anisotropies in Cu(110) an Au(110) could have their origin from the reduced symmetry of the (110) surface. A similar qualitative conclusion has been traced back from our earlier calculation<sup>25</sup> on the optical properties of Ag(110). The transitions take place between parallel energy bands not necessary horizontal, and they do not take place always near high-symmetry points. At low energy a major contribution to these anisotropies comes from ( $sp \rightarrow sp$ ) involving generally ( $S$ ) and ( $S-1$ ) surfaces, and beyond 2.0 eV the contribution from occupied  $d$  bands is enhanced and the deeper layer ( $S-2$ ) is more implicated.

#### IV. CONCLUSION

According to our analysis of the calculated optical spectra of Cu and Au(110) surfaces we can conclude that interband transitions do not occur only between bands that give high-density region (i.e., bands with zero gradients) and they are not limited to high-symmetry directions. The transitions may occur anywhere in the BZ when the two involved bands have the same gradients and the corresponding transitions are allowed by the selection rules. The band structures presented here are only a partial representation of a global situation. Parallel bands that contribute to the transition may be found in other directions which are not necessarily close to high-symmetry points. We can also conclude that for noble-metal

(110) surfaces, the interband transitions inducing the anisotropy are surface effects and can occur mainly in surface ( $S$ ), subsurface ( $S-1$ ), and sub-subsurface ( $S-2$ ) atomic layers. They are not limited only to high-symmetry points or to high-density regions. For low photon energies, the dominant part of the transitions is of type ( $sp \rightarrow sp$ ) and ( $sd \rightarrow p$ ). The contribution from pure  $d$  bands becomes important only for high-energy range.

## ACKNOWLEDGMENTS

We gratefully acknowledge M. A. Khan for his help as well as for his useful and stimulating discussions. This work was supported by Algerian Project ANDRU/PNR3 (AU4 499 02) and by collaborative programs DEF/CNRS (SPM 12329) between the University Louis Pasteur of Strasbourg, France, and the University Mouloud Mammeri of Tizi-Ouzou, Algeria.

- <sup>1</sup>W. Richter and J.-T. Zettler, Appl. Surf. Sci. **100/101**, 465 (1996).
- <sup>2</sup>*Epioptics: Linear and Nonlinear Optical Spectroscopy of Surfaces and Interfaces*, edited by J. F. McGilp and D. Weaire (Springer, Berlin, 1995).
- <sup>3</sup>Y. Borensztein, W. L. Mochan, J. Tarriba, R. G. Barrera, and A. Tadjeddine, Phys. Rev. Lett. **71**, 2334 (1993).
- <sup>4</sup>A. Borg, O. Hunderi, W. Richter, J. Rumberg, and H. J. Venvik, Phys. Status Solidi A **152**, 77 (1995).
- <sup>5</sup>S. M. Scholz, F. Mertens, K. Jacobi, R. Imbihl, and W. Richter, Surf. Sci. Lett. **340**, 945 (1995).
- <sup>6</sup>Ph. Hofmann, K. C. Rose, V. Fernandez, A. M. Bradshaw, and W. Richter, Phys. Rev. Lett. **75**, 2039 (1995).
- <sup>7</sup>V. Fernandez, D. Pahlke, N. Esser, K. Stahrenberg, O. Hunderi, A. M. Bradshaw, and W. Richter, Surf. Sci. **377-379**, 388 (1997).
- <sup>8</sup>B. G. Frederick, J. R. Power, R. J. Cole, C. C. Perry, Q. Chen, S. Haq, Th. Bertrams, N. V. Richardson, and P. Weightman, Phys. Rev. Lett. **80**, 4490 (1998).
- <sup>9</sup>K. Stahrenberg, T. Herrmann, N. Esser, J. Sahn, W. Richter, S. V. Hoffmann, and Ph. Hofmann, Phys. Rev. B **58**, 10 207 (1998).
- <sup>10</sup>J.-K. Hansen, J. Bremer, and O. Hunderi, Surf. Sci. **418**, L58 (1998).
- <sup>11</sup>J. Bremer, J.-K. Hansen, and O. Hunderi, Surf. Sci. **436**, L735 (1999).
- <sup>12</sup>K. Stahrenberg, Th. Herrmann, N. Esser, and W. Richter, Phys. Rev. B **61**, 3043 (2000).
- <sup>13</sup>K. Stahrenberg, Th. Herrmann, N. Esser, W. Richter, S. V. Hoffmann, and Ph. Hofmann, Phys. Rev. B **65**, 035407 (2001).
- <sup>14</sup>J. Woll, G. Meister, U. Barjenbruch, and A. Goldmann, Appl. Phys. A: Mater. Sci. Process. **60**, 163 (1995).
- <sup>15</sup>K. Stahrenberg, Th. Herrmann, N. Esser, and W. Richter, Phys. Rev. B **61**, 3043 (2000).
- <sup>16</sup>M. J. Jiang, G. Pajer, and E. Burstein, Surf. Sci. B **242**, 306 (1991).
- <sup>17</sup>A. I. Shkrebtii, N. Esser, W. Richter, W. G. Schmidt, F. Bechstedt, B. O. Fimland, A. Kley, and R. Del Sole, Phys. Rev. Lett. **81**, 721 (1998).
- <sup>18</sup>U. Rossow, L. Mantese, and D. E. Aspens, J. Vac. Sci. Technol. A **14**, 3070 (1996).
- <sup>19</sup>Y. Borensztein, W. Roy, and R. Alameh, Europhys. Lett. **31**, 331 (1995).
- <sup>20</sup>W. L. Mochan, R. G. Barrera, Y. Borensztein, and A. Tadjeddine, Physica A **207**, 334 (1994).
- <sup>21</sup>J. K. Hansen, J. Bremer, and O. Hunderi, Phys. Status Solidi A **170**, 271 (1998).
- <sup>22</sup>P. T. Feibelman, Prog. Surf. Sci. **12**, 287 (1982).
- <sup>23</sup>M. Mebarki, A. Ziane, S. Bouarab, and M. A. Khan, Surf. Sci. **454-456**, 433 (2000).
- <sup>24</sup>P. Monachesi, M. Palummo, R. Del Sole, R. Ahuja, and O. Eriksson, in *Optical Properties of Materials*, edited by J. R. CheLIKowsky, S. G. Louie, G. Martinez, and E. L. Shirley, Mater. Res. Soc. Symp. Proc. No. 579 (Materials Research Society, Pittsburgh, 2001), p. 59.
- <sup>25</sup>S. Bouarab, M. Mebarki, A. Ziane, and M. A. Khan, Phys. Rev. B **63**, 195409 (2001).
- <sup>26</sup>Patrizia Monachesi, Maurizia Palummo, Rodolfo Del Sole, Rajeev Ahuja, and Olle Eriksson, Phys. Rev. B **64**, 115421 (2001).
- <sup>27</sup>M. Rohlfing and S. G. Louie, Phys. Rev. Lett. **83**, 856 (1999), and references therein.
- <sup>28</sup>P. H. Hahn, W. G. Schmidt, and F. Bechstedt, Phys. Rev. Lett. **88**, 016402 (2001), and references therein.
- <sup>29</sup>S. Albrecht, L. Reining, R. Del Sole, and G. Onida, Phys. Rev. Lett. **80**, 4510 (1998), and references therein.
- <sup>30</sup>R. Kofman, P. Cheyssac, and J. Richard, Surf. Sci. **77**, 537 (1978).
- <sup>31</sup>Y. Borensztein, W. L. Mochan, J. Tarriba, R. G. Barrera, and A. Tadjeddine, Phys. Rev. Lett. **71**, 2334 (1993).
- <sup>32</sup>V. Mazine, Y. Borensztein, L. Cagnon, and P. Allongue, Phys. Status Solidi A **175**, 311 (1999).
- <sup>33</sup>B. Sheridan, D. S. Martin, J. R. Power, S. D. Barrett, C. I. Smith, C. A. Lucas, R. J. Nichols, and P. Weightman, Phys. Rev. Lett. **85**, 4618 (2000).
- <sup>34</sup>R. W. G. Wyckoff, *Crystal Structures*, 2nd ed. (Interscience, New York, 1963).
- <sup>35</sup>C. Koenig and M. A. Khan, Phys. Rev. B **27**, 6129 (1983).
- <sup>36</sup>O. Jepsen and O. K. Andersen, Solid State Commun. **9**, 1763 (1971).
- <sup>37</sup>O. K. Andersen, Phys. Rev. B **12**, 3060 (1975).
- <sup>38</sup>H. L. Skriver, *The LMTO Method* (Springer, Berlin, 1984).
- <sup>39</sup>U. von Barth and L. Hedin, J. Phys. C **5**, 1629 (1972).
- <sup>40</sup>M. A. Khan, Appl. Surf. Sci. **66**, 18 (1998).